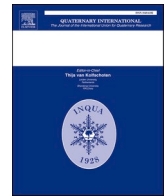




Contents lists available at ScienceDirect

Quaternary International

journal homepage: www.elsevier.com/locate/quaint

Speleothem growth phases in the central Eastern Desert of Egypt reveal enhanced humidity throughout MIS 5

Felix Henselowsky^{a,b,*}, René Eichstädter^c, Andrea Schröder-Ritzrau^c, Daniel Herwartz^d, Ahmed Almoazamy^e, Norbert Frank^{c,g}, Karin Kindermann^{a,f}, Olaf Bubenzer^{a,b,g}

^a CRC 806 „Our Way to Europe“, University of Cologne, Bernhard-Feilchenfeld-Str. 11, 50969, Cologne, Germany

^b Institute of Geography – Heidelberg University, Im Neuenheimer Feld 348, Heidelberg, Germany

^c Institute of Environmental Physics – Heidelberg University, Im Neuenheimer Feld 229, Germany

^d Institute of Geology and Mineralogy, University of Cologne, Zùlpicher Str. 49b, 50674, Cologne, Germany

^e Egyptian Mineral Resource Authority (EMRA), Salah Salem Street 3, Abbasiya, Cairo, Egypt

^f Institute of Prehistoric Archaeology, African Archaeology, University of Cologne, Bernhard-Feilchenfeld-Str. 11, 50969, Cologne, Germany

^g Heidelberg Center for the Environment - Heidelberg University, Im Neuenheimer Feld 360, Heidelberg, Germany

ARTICLE INFO

Keywords:

Last Interglacial
Northeast Africa
Palaeoclimate
Speleothems
Uranium-series dating
Homo sapiens dispersal

ABSTRACT

Speleothem deposits in nowadays arid environments are important climate archives, as they indicate phases of enhanced precipitation and can precisely be dated by uranium-series dating. So far only very few of such archives have been found in the today hyper-arid Saharo-Arabian Desert (SAD). Therefore, the study at hand fills a gap that exists for speleothem climate archives in Northeast Africa. A new record from Saqia Cave (Central Eastern Desert, Egypt) documents for the first-time speleothem growth in Egypt for all sub-stages of MIS 5 and singular phases during MIS 6. Most important growth phases occur during periods of strong increase and maximum orbitally-forced northern hemisphere insolation, but also during phases of low insolation, which are in general attributed to aridity in North Africa. Here, at least semi-arid climate conditions are proposed for periods of low insolation during stadials of MIS 5. This suggests an impact of different possible sources of precipitation, apart from large scale shifts of the African monsoon, such as Red Sea Troughs, tropical plums and a larger spatial extent of the Mediterranean winter-rainfall zone.

Concerning the spatial rainfall pattern in Egypt, we propose a considerable east to west rainfall gradient in Egypt for the Last Interglacial and suggest a stronger impact of variable moisture sources in the Eastern Desert near the Mediterranean and Red Sea in comparison to the more continental Western Desert of Egypt. This reveals more favorable pre-conditions for an enhanced land use potential in the past. Therefore, the more sustaining wetter climate in the Eastern Desert point to a recurring feasible dispersal corridor for *Homo sapiens* from the tropical climate into the temperate climate regime throughout MIS 5. Such a more humid climate provided an ideal basis for long-term, favorable environmental conditions east of the Nile Valley, creating a kind of contiguous landscape corridor that may have been attractive to humans and wildlife alike, linking the East African tropical climate regime with that of the temperate zone in Northeast Africa and Eurasia.

1. Introduction

Northeast Africa provides the only terrestrial dispersal route for humans from the African continent into Eurasia. This land route crosses the nowadays largest continuous hyper-arid zone in the world, the Saharo-Arabian Desert (SAD). Therefore, a better understanding of palaeoenvironmental changes and an identification of formerly wetter climate phases with more favorable ecological conditions is of high

relevance for the understanding and the reconstruction of potential human dispersal routes Out of Africa (OoA). Climate models indicate that North Africa was in general wetter during the peak of the Last Interglacial (LIG) at MIS 5e (cf. Jennings et al., 2015; Kutzbach et al., 2014). Indeed, marine records from the Mediterranean Sea point to wetter climate with strong freshwater influx into and high activity of North African wadis during sub-stages MIS 5e, c and a, but more arid conditions during MIS 5d and 5b (cf. Rohling et al., 2015; Ehrmann

* Corresponding author. Institute of Geography – Heidelberg University, Im Neuenheimer Feld 348, Heidelberg, Germany.

E-mail address: felix.henselowsky@uni-heidelberg.de (F. Henselowsky).

<https://doi.org/10.1016/j.quaint.2021.05.006>

Received 20 February 2021; Received in revised form 9 April 2021; Accepted 6 May 2021

Available online 15 May 2021

1040-6182/© 2021 The Authors. Published by Elsevier Ltd. This is an open access article under the CC BY license (<http://creativecommons.org/licenses/by/4.0/>).

et al., 2016; Grant et al., 2017). The wetter phases are in general associated with an increase and peaks of orbitally-forced insolation at precession time scales. Similar to climate modelling the marine records, e.g. in the Eastern Mediterranean Sea, integrate palaeoenvironmental information also over large catchment areas (e.g. the Nile catchment). Addressing regional to local characteristics from terrestrial records, however, allows better to understand the tempo-spatial heterogeneity of these climate changes. This smaller scale can actually discuss the distinct environmental context by integrating archaeological sites. Therefore, terrestrial climate archives in the SAD are crucial, even though their spatial distribution is rare and their preservation is often poor. Moreover, their temporal resolution and proxy data are often not as detailed as the marine records from the surrounding regions of the Red Sea and the Mediterranean Sea.

Speleothems, which can be precisely dated using uranium series dating, are an excellent regional climate archive but rare terrestrial archives in arid environments. In arid regions, their growth phases indicate wetter climate conditions with positive effective precipitation (Bar-Matthews et al., 2019). This is associated with vegetation growth and the production of soil CO₂, which causes dissolution of carbonate in limestone host rocks and the enhanced effective infiltration of water lead to subsequent deposition of secondary carbonates when CO₂ degasses (Ford and Williams, 2007). These deposits are very limited in the SAD and were identified as a lack of knowledge in Northeast Africa (Braun et al., 2019). Until now, speleothem growth during the LIG in Egypt is only documented at Wadi Sannur Cave (Eastern Desert) and Djara Cave (Western Desert; Brook et al., 2002; Dabous and Osmond, 2000; El-Shenawy et al., 2018). Other records are so far mainly known



Fig. 1. A) Overview of Gebel Duwi and studied archive at Saqia Cave (1) with archaeological sites (2: Sodmein Cave, 3 Sodmein Playa) mentioned in the text. LANDSAT 8 (U.S. Geological Survey products, Bands 2, 3, 4), Index-map MODIS- satellite image (Stöckli et al., 2005.) B) Field view of Saqia Cave and flowstone deposits with positions of cores Saqia 1–4.

from the northern margins of the SAD in the southern Negev Desert, Israel (Vaks et al. 2007, 2010) or at its southern boundary in Yemen, Mukalla Cave (Burns et al. 1998, 2011; Fleitmann et al., 2003) and Hoti Cave in Oman (Fleitmann et al., 2011).

Here, we present uranium-series dating including its isotope composition of $\delta^{13}\text{C}$ and $\delta^{18}\text{O}$ of a speleothem from Saqia Cave, located in the Central Eastern Desert of Egypt. Presently, no speleothem growth occurs in this region due to the hyper-arid climate. Thus, speleothem growth is restricted to wetter climate phases in the Eastern Desert and the dating of these growth phases allows the identification of climate changes in the past.

The climate record contributes to a better understanding of regional human occupations associated with wetter climate and possible migrations towards the southern Levant. Importantly, the results can be linked to the occupation at the nearby archaeological sites of Sodmein Cave and Sodmein Playa (Kindermann et al., 2018). Sodmein Cave is located only about 10 km apart from Saqia Cave and is one of the few Late Pleistocene living sites in Northeast Africa. In consequence, this setting provides a unique opportunity to compare a terrestrial climate archive with an archaeological site in direct context to each other and in one of the key regions for human dispersal OoA.

2. Study area and sites of investigations

Saqia Cave (26°19'43"N, 33°54'18"E) is located in the Central Eastern Desert of Egypt at the hogback of Gebel Duwi (Fig. 1a), which consists of Cretaceous to Eocene limestone, marls and shales (Khalil and McClay, 2002). The cave itself is situated within the lower Eocene Thebes formation, which consists of chalky and dolomitic limestone with abundant flint bands (Conoco 1987; Yousif et al. 2018). The elevation above current Red Sea Level is 210 m and airline between Saqia and the Red Sea is about 25 km. Current precipitation in the area is almost absent with an average of 3.5 mm annual rainfall from 1985 to 2014, with very rare single rainfall events (12 between 1945 and 2010) having a maximum of 27 mm (Yousif and Sracek, 2016). Data on modern day isotope composition of rainfall are very limited in the area with the given isolated rainfall events. Limited data exist only for the slightly wetter Mediterranean coast of Egypt, which accounts for modern mainly eastern Mediterranean precipitation source during winter times. Here, monthly values of $\delta^{18}\text{O}$ ranges from -4% to -1.8% (El-Asrag, 2005).

The cave consists of a small cavity, which is incised into the Thebes limestone. Today, the cave entrance is blocked by sand accumulation. A massive flowstone is deposited at around 4–6 m above the cavity (Fig. 1b). The flowstone has a diameter of approximately 27 cm at its central part and a height of around 2–3 m. The upper part is consisting of the actual flowstone and the lower part consists of an additional overflow of secondary carbonates at the bottom of the bedrock. Post-depositional strains has led to a crack at the backside of it. The overlain surface catchment from above the limestone has an area of 0.15 km², which represents a very small surface catchment for the flowstone. Additional water influx from the surrounding permeable and karstified limestone cannot be excluded. However, the amount of such water surplus is suspected to be small, as the overlain limestone is only few meters thick and the inclination of the limestone layers limits the possible subterranean catchment. Groundwater influence is not possible due to the elevated position of the flowstone. Therefore, the local rainfall generated the water source for the flowstone, which preserved an archive of the regional to local precipitation in the past.

3. Methods

Sampling of the speleothem was done with a wet core diamond drill (Weka DK12), using a 20 mm tube for the collection of cores. Drillings were performed at the central part of the flowstone horizontally crossing of the expected stratigraphy (Saqia_1) and at the bottom of

the flowstone, where the secondary carbonates cover the bedrock (Saqia_4). Two additional cores were drilled subsequently after the initial dating's of core 1 gave the most promising results. They were drilled 6 cm (Saqia_2) and 10 cm (Saqia_3) below the first core up to the central part of the flowstone.

Uranium-series dating was conducted at the Institute for Environmental Physics at Heidelberg University. Sample preparation and measurements were done after the method described in Douville et al., (2010) and Wefing et al., (2017). Chemical Th and U separation and purification is based on ion exchange processes using UTEVA resin following sample dissolution. Subsequently, isotope ratios were measured using either thermal ionisation mass spectrometry (TIMS, Finnigan MAT 262 RPQ) according to the method described in Frank et al. (2000), or by multi-collector inductively coupled-plasma mass spectrometry (MC-ICPMS, Thermo Scientific Neptune Plus) following the procedure of Wefing et al., (2017). Isotope ratios were then used to estimate U-series ages according to the decay equations (Ludwig and Titterton, 1994) and by means of the half-life values of ²³⁴U and ²³⁰Th published by Cheng et al., (2000).

Measurement of $\delta^{13}\text{C}$ and $\delta^{18}\text{O}$ have been conducted for Saqia_1 and two samples from Saqia_2. Due to the complex growth axis and missing secure age information for the undated sections, the $\delta^{13}\text{C}$ and $\delta^{18}\text{O}$ is only related to the distinct sampling sections, where definitive Th/U-ages exist.

Carbonate isotope analyses were performed using a KIEL IV carbonate device connected to a MAT253 gas mass spectrometer installed at the Institute for Geology and Mineralogy in Cologne. The internal precision for replicates of ca. 60 µg dry carbonate powder was 0.06‰ for both $\delta^{13}\text{C}$ and $\delta^{18}\text{O}$, well below the typical external reproducibility of 0.1‰. Accepted isotope values for the standard materials NBS18 and NBS19 measured along with the samples were used to bring all analyses on the VPDB scale (Meier-Augenstein and Schimmelmann, 2019). Accuracy was confirmed via analyses of another in house carbonate standard (Carrara).

4. Results

The uranium-series-dating for the flowstone at Saqia Cave show 21 ages ranging between 185.7 ± 4.3 ka to 83.2 ± 2.1 ka with most of the dating (18 out of 21) falling into MIS 5 (Table 1). Temporally isolated evidence for speleothem growth phases during MIS 6 are shown at 185.7 ± 4.3 ka, 174.0 ± 4.6 ka, 155.6 ± 3.9 ka.

The dated growth phases for the three cores from Saqia Cave reveals that the internal structure of the flowstone and growth axis are complex (Fig. 2). Ages show a decrease from the right outer side towards its inner part up to 17 cm. Saqia_1 has an abrupt increase in age in the section 17.5 to 18 cm, showing an age inversion from 85.48 ± 0.40 ka to 185.8 ± 4.3 ka. From 18.3 cm onwards, the deposits are younger towards the left side of the flowstone. Cores Saqia_2 and Saqia_3, situated 4 and 10 cm above core Saqia_1, are comparable with the oldest ages at its inner side (right) and younger ages towards the central part (left). As these cores are only cored up to the central part, the observed age inversion at the very left side is not recorded in these cores. Saqia_3 has one age outlier at 5.8 cm with an age of 114.5 ± 2.2 ka. All other ages are stratigraphically in order within their 2σ error, e.g. Saqia_1 at 7.5 cm with 96.7 ± 2.7 ka and at 4.5 cm with 99.1 ± 2.3 ka. U concentrations are between 300.16 ± 0.56 ng and 1380.1 ± 1.4 ng and all samples show elevated ²³²Th concentrations. ²³⁰Th/²³²Th activity ratios of 106 on average result in moderate age correction due to ²³²Th content and age errors between 0.39 ka and 4.6 ka, respectively.

Although a detailed age-depth model cannot be established based on this stratigraphy, the interpretation of growing phases can reveal insights into the onset and offset of secondary carbonate deposition after enhanced precipitation, vegetation growth and soil CO₂ production.

Results for $\delta^{13}\text{C}$ and $\delta^{18}\text{O}$ (Table 2) account for the isotope composition of each dated section and reveal insights into the moisture source

Table 1

Results for calculated ages for Saqia Cave. All measurements and absolute concentrations of Th and U are given in appendix 1. * corrected age; corrected for detrital Th; assuming bulk Earth $^{232}\text{Th}/^{238}\text{U}$ weight ratio of 3.8 ± 1.9 for detritus and ^{234}U , ^{238}U and ^{230}Th in secular equilibrium.

Massspectrometer used for analysis	Dating performed in	Lab. No.	sample ID	depth [cm]	Age [ka]	Age * [ka]	MIS stage
ICP-Q-MS	2014	IUP-6435	Saqia1-1,7	1.7	133.5 ± 2.0	127.2 ± 3.5	5e/6
ICP-Q-MS	2014	IUP-6436	Saqia1-6,0	6	127.7 ± 2.8	127.1 ± 2.8	5e
ICP-Q-MS	2014	IUP-6437	Saqia1-11,5	11.5	124.9 ± 1.8	124.5 ± 1.8	5e
MC-ICPMS	2018	IUP-9180	Saqia1-13,0	13.0	110.32 ± 0.55	110.03 ± 0.55	5d
MC-ICPMS	2018	IUP-9181	Saqia1-15,0	15.0	110.85 ± 0.39	110.72 ± 0.39	5d
MC-ICPMS	2018	IUP-9182	Saqia1-17,0	17.0	85.84 ± 0.28	85.48 ± 0.40	5a/b
ICP-Q-MS	2014	IUP-6438	Saqia1-18,3	18.3	186.21 ± 4.3	185.7 ± 4.3	6
ICP-Q-MS	2014	IUP-6439	Saqia1-23,7	23.7	174.8 ± 4.6	174.0 ± 4.6	6
ICP-Q-MS	2014	IUP-6440	Saqia1-26,7	26.7	156.8 ± 4.0	155.6 ± 4.0	6
MC-ICPMS	2018	IUP-9177	Saqia2-1,0	1.0	121.41 ± 0.70	120.57 ± 0.75	5e
MC-ICPMS	2018	IUP-9178	Saqia2-5,0	5.0	106.41 ± 0.72	105.87 ± 0.72	5c/d
MC-ICPMS	2018	IUP-9179	Saqia2-10,0	10.0	90.84 ± 0.35	90.23 ± 0.45	5b
TIMS	2012/2013	IUP-5946	Saqia_3-1	1	105.8 ± 2.1	105.2 ± 2.2	5d/e
TIMS	2012/2013	IUP-5787	Saqia_3-3,8	3.8	104.1 ± 3.6	103.8 ± 3.6	5c/d
TIMS	2012/2013	IUP-5912	Saqia_3-7,5	7.5	98.1 ± 2.6	96.7 ± 2.7	5c/d
TIMS	2012/2013	IUP-5945	Saqia_3-9,2	9.2	115.5 ± 2.2	114.5 ± 2.2	5d/e
TIMS	2012/2013	IUP-6004	Saqia_3-10,5	10.5	100.0 ± 2.3	99.1 ± 2.3	5c
TIMS	2012/2013	IUP-5911	Saqia_3-11,5	11.5	85.7 ± 1.8	85.4 ± 1.8	5a/b
TIMS	2012/2013	IUP-5786	Saqia_3-12,8	12.8	84.4 ± 2.0	83.2 ± 2.1	5a/b
TIMS	2012/2013	IUP-5913	Saqia_4-2	2	121.3 ± 2.3	119.7 ± 2.4	5e
TIMS	2012/2013	IUP-5788	Saqia_4-13	13	86.1 ± 2.1	84.4 ± 2.2	5a/b

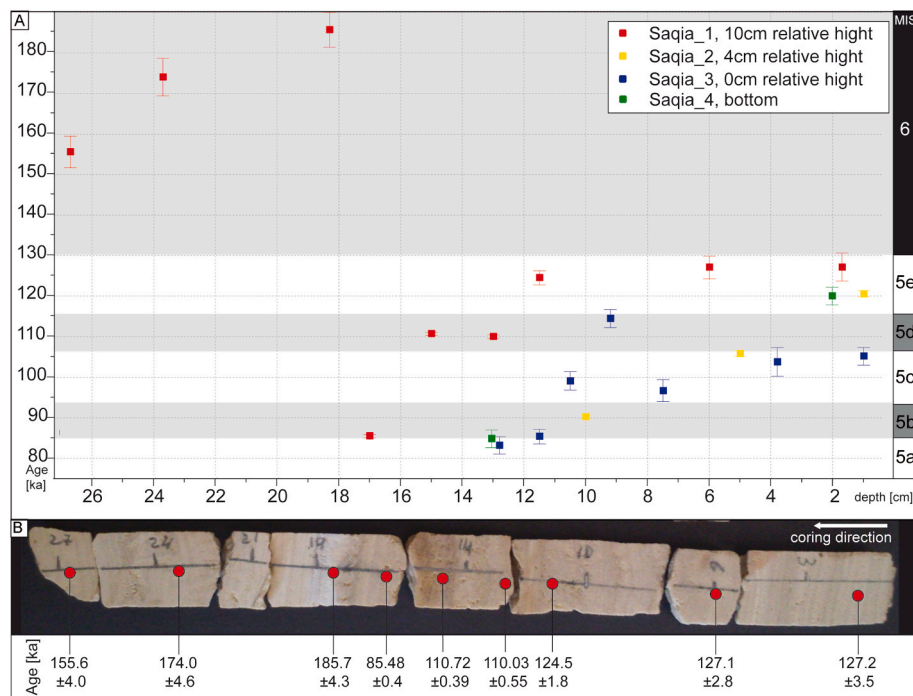


Fig. 2. A) Age-depth plot for Th-U dating results from Saqia Cave and B) image with stratigraphy of sample Saqia_1.

Table 2

Results for mean values of $\delta^{13}\text{C}$ and $\delta^{18}\text{O}$ for samples from Saqia_1 and Saqia_2.

Sample ID	Age	± [ka]	$\delta^{18}\text{O}$ Mean	$\delta^{13}\text{C}$ Mean
S1-1,7	127.2	3.5	-11.08	-6.01
S1-6	127.1	2.8	-10.97	-5.09
S1-11,5	124.5	1.8	-11.55	-5.37
S1-13	110.03	0.55	-10.90	-4.86
S1-15	110.72	0.39	-10.97	-7.60
S1-17	85.48	0.4	-11.34	-2.58
S1-18,3	185.7	4.3	-11.73	-7.07
S1-23,7	174	4.6	-11.31	-6.33
S1-26,7	155.6	4.0	-11.03	-6.60
S2-1	120.57	0.75	-10.90	-6.63
S2-5	105.87	0.72	-11.06	-3.78

in the Eastern Desert and possible changes in the dominance of C3/C4 type vegetation. $\delta^{18}\text{O}$ ranges between -10.90‰ and -11.73‰ with a mean of $-11,22 \pm 0,29\text{‰}$. Overall, variations between individual sub-stages of MIS 5 are limited. $\delta^{13}\text{C}$ is more variable ranging between $-2,58\text{‰}$ and $-7,07\text{‰}$ with a mean value of $-5,67 \pm 1,2\text{‰}$. $\delta^{13}\text{C}$ values during MIS 5e are lower during MIS 5e and higher during MIS 5d and 5b, although absolute lowest $\delta^{13}\text{C}$ values from one sample of $-7,6\text{‰}$ exists during MIS 5d.

5. Discussion

The presence and absence of speleothem deposition in (hyper-) arid environments can be regarded as an on-off situation. Deposition take place during phases of sufficient water availability and vegetation

growth ("on"), whereas speleothem growth is absent under an arid climate ("off"). Hence, the dated speleothem growth phases at Saqia indicate wetter climate conditions and can be compared to speleothem growth phases known from other sites in the SAD, but also with climate modelling data and the marine records. Thereby, our regional terrestrial climate archives provide insights into the spatial heterogeneity of environmental settings in Northeast Africa during the LIG.

First of all, the identified growth phases and the inversion of ages within the stratigraphy of Saqia_1 at around 18 cm indicates that the dripline of secondary carbonate deposition changed throughout the sequence. So far, it is unclear why the ages follow from older to younger ages from the right-hand side towards its central part with the distinct inversion from the central part towards the left part. This growth direction (here seen as left to right) for the growth phases during MIS 5, is consistent in all cores and thus represents the actual growth direction. It is possible that these younger deposits had filled up an old crack within the flowstone and that the two sections are previously separated and the MIS 6 section had another growth direction. All younger deposits dated to MIS 5 are subsequent deposited up to the contact of the older carbonates. The flowstone has no continuous contact to the bedrock at its back. Such cracks certainly have an influence on secondary carbonate deposition. The crack at the back is presumable old and the dripline of water may have changed towards the inner part of the flowstone over prolonged time periods. Such a depositional change is also visible in the lithology of the core (Fig. 2b), where a distinct change in color occurs between 17 and 18 cm in Saqia_1. The fact that different ages occur on the same depth of the different cores reveal insights that the age-depth of the flowstone is not linear in a vertical dimension. Complex and bi-directional growth is a common feature and challenge in discontinuous speleothem growth, particular in arid environments (Burstyn et al., 2019).

Even though the detailed growth axes have changed throughout the deposition, the boundary factors and the context of the flowstone itself persists through the timescale of interest. It is assumed that the small overlain surface catchment above the cavity did not change tremendously since MIS 5. The low coverage of overlain limestone does not imply a considerable effect of karst-hydrological features and geomorphological setting does not indicate any significant relief changes throughout the late Pleistocene. This observation is consistent with the low seismicity in the broader area (Sawires et al., 2016) and implies that tectonic activity related to the Red Sea rift system (Khalil and McClay, 2002) was unimportant and that the recent morphology provides the general morphological framework for the timescale of interest (Yousif et al. 2018). However, very local events such as earthquakes and surface ruptures that may have changed water driplines cannot be excluded.

Detailed studies in the Negev Desert have defined the precipitation limit for speleothem deposits there. Minimum of 200–275 mm/a was required for speleothem deposition during glacial periods, whereas during the interglacials 300–350 mm/a is required (Vaks et al., 2010). Thus, speleothem deposits represent not only the actual net precipitation, but also the effective available precipitation, which can change throughout time with temperature and the variable course of rainfall seasons throughout the year (summer rainfall with higher temperature or winter rainfall with lower temperature). Based on the comparison with the Negev Desert speleothems, the dated growth phases from Saqia Cave point to a minimum precipitation of 300 mm/a in the Eastern Desert, which is in tremendous contrast to the nowadays hyper-arid climate with less than 50 mm precipitation per annum. However, the actual precipitation during growth phases may have been much higher than the minimum of 300 mm/a. Due to its geographical position, present and past temperature and insolation in the Eastern Desert of Egypt is higher than in the Levant indicating that higher precipitation is needed for effective carbonate dissolution, because the portion of evaporation loss without reaching the unsaturated zone is higher. The archaeobotanical and -zoological analyses of Sodmein Cave, located only a few kilometers apart from Saqia Cave, show that during the peak

of the LIG at stage MIS 5e the region was associated with a savannah-like environment and annual precipitation of up to 600 mm (Moeyersons et al., 2002).

The absence of speleothem growth after MIS 5 constitutes no absolute evidence of absence of a wetter climate in the Eastern Desert during MIS 4 and 3. It is also possible that wetter climate during MIS 4 was not as pronounced as in MIS 5 and the specific threshold for the deposition of secondary carbonates was not reached. This is a common feature seen in discontinuous speleothem records, in particular in environments with water limited climate (Burstyn et al., 2019). Based on the numerous pre-conditions for successful speleothem growth, in particular for arid environments, it is not obvious that enhanced precipitation during wetter climate phases are directly associated with starting speleothem growth. Short-term rainfall events and flash-floods might create a distinct sedimentological signature, e.g. shown in marine records of the Red Sea (Hartmann et al., 2020). If this signature is persistent over a longer time, it is an argument for a wetter climate, whereas the actual precipitation predominantly falls in heavy, but short events. Enhanced precipitation of single events does not necessarily create speleothem growth, as the process of secondary carbonate deposition occurs during phases of longer moisture availability (vegetation growth, enhanced soil CO₂, dissolution and deposition of carbonates). Therefore, signals from marine records for a wetter climate during MIS 4 (e.g. Ehrmann et al., 2016) does not need to be obligatory present in our record. Due to the complex growth direction of the flowstone, it is also possible that growth phases during MIS 4 and 3 are not sampled, as the drip line changed. Thus, all dated growth phases from Saqia Cave represent the minimum time periods of enhanced precipitation in the Eastern Desert of Egypt.

5.1. Comparison with other speleothem deposits in the SAD

The spatial distribution of speleothem research is restricted to a few sites at the margins of the SAD. The Saharan belt itself is almost unstudied hindering any detailed regional comparison.

In context of regional comparisons with speleothem deposits in the SAD, Saqia Cave reveals the most abundant growth phases in time (Fig. 3). Central and southern Negev Desert speleothems have only episodic deposition, very thin laminae and the sites are highly dispersed (Vaks et al., 2010, Bar-Matthews et al., 2019). Most of them are comparable to Saqia Cave in view of their discontinuous records, where not only changing water availability, but also complex structures of both, stalagmites, stalactites and flowstones lack any simple in-depth stratigraphy's, e.g. for continuous stable isotope records. In Egypt, Wadi Sannur Cave (northern Eastern Desert) reveals speleothem growth phases mainly during MIS 5e with only one dating that falls into MIS 5d and one into MIS 4 respectively, suggesting that other sub-stages of MIS 5 had been too dry for speleothem deposition at Sannur Cave (Dabous and Osmond, 2000; El-Shenawy et al., 2018). However, the absence of evidence also cannot be interpreted as an absolute criterion for a dry climate. At Djara Cave (Western Desert) one U/Th date of 140 ± 16 ka exists (Brook et al., 2002).

At the southern limit of the SAD, speleothem growth in two caves on the Arabian Peninsula Hoti Cave (Oman) and Mukalla Cave (Yemen) reveal a wetter climate during the Late Pleistocene (Fleitmann et al., 2011), mainly during MIS 5e/d and MIS 5a. Growth periods in the southern Negev Desert (Vaks et al., 2010) cluster in MIS 5e with little occurrences following into MIS 5d. So far, only one age exists apart from this cluster. Even-Sid caves indicating speleothem growth during MIS 5b, but no records exist which show growth periods in the southern Levant between 109 and 89 ka (Vaks et al., 2010). The records from Mukalla Cave (Yemen) and Hoti Cave (Oman) show similar patterns with the main deposition during MIS 5e/d and additional deposits during MIS 5a (Fleitmann et al., 2011). Thus, most speleothem growth dates indicate wetter climate phases during the LIG to MIS 5e (summary in Bar-Matthews et al., 2019).

The $\delta^{13}\text{C}$ isotope composition from Saqia Cave is much more

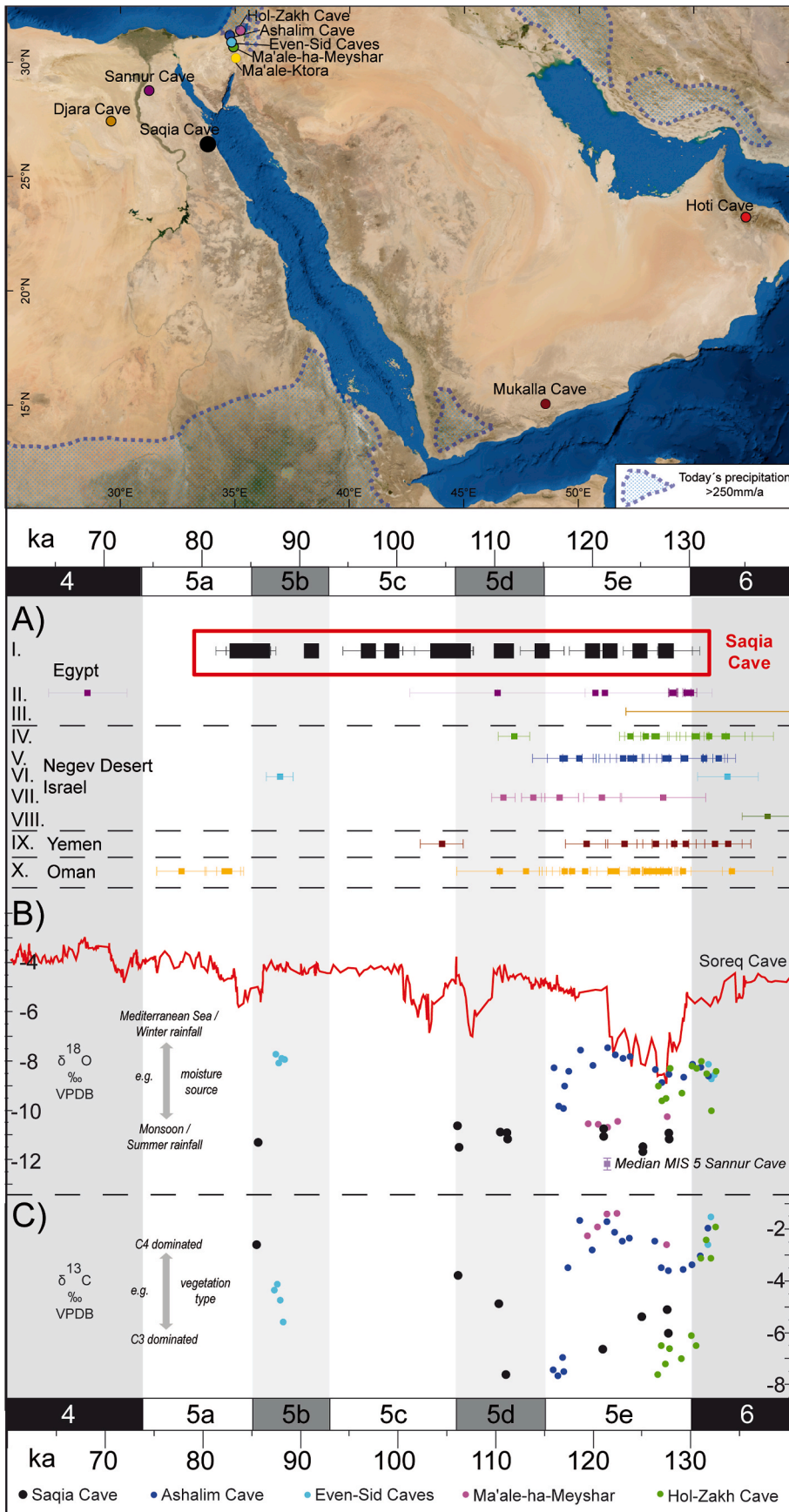


Fig. 3. A) speleothem growth in the SAD: Eastern Desert of Egypt, I. Saqia Cave (black square, this study); II. Sannur Cave (Osmond & Dabous 2004; El-Shenawy et al., 2018); Western Desert of Egypt, III. Djara Cave Brook et al., 2002); Negev Desert, Israel, IV. Hol-Zakh Cave, V. Ashalim Cave, VI. Even-Sid Caves, VII. Ma'ale-ha-Meyshar, VIII. Ma'ale-Ktora, (Burns et al. 1998, 2011; Vaks et al., 2010); Yemen, IX. Mukalla Cave; Oman, X. Hoti Cave (Fleitmann et al. 2003, 2011); B) and C) $\delta^{18}\text{O} / \delta^{13}\text{C}$ from Saqia Cave (this study); Soreq Cave, Grant et al., (2012); Sannur Cave, El-Shenawy et al., (2018); Negev Desert Vaks et al., 2010). MIS-stages are indicated at the top and bottom according to Railsbeck et al., (2015).

heterogeneous and variable in comparison to $\delta^{18}\text{O}$. This is a typical feature for speleothems in general (e.g. Bajo et al., 2017) and also observed for the speleothem deposits of the Levant, where $\delta^{13}\text{C}$ show complicated features (Bar-Matthews et al., 2019). Several sources of carbon (C3 and C4 plants, bedrock) are mixed to variable degrees and isotope fractionation, e.g. due to CO_2 degassing or prior calcite precipitation, generates isotopic variability that is superimposed on the source variability (Bajo et al., 2017). Hence, the effective $\delta^{13}\text{C}$ composition depends on parameters such as the C component of the host rock, soil $p\text{CO}_2$, soil cover thickness, soil biological activity, evaporation and degassing (Bajo et al., 2017). These complexities hinder a straight forward interpretation of $\delta^{13}\text{C}$ values in terms of C3/C4 vegetation (Vaks et al., 2010, Bar-Matthews et al., 2019). Nevertheless, the following comparison of speleothem $\delta^{13}\text{C}$ values in the broader region, combined with Archaeological evidence provides some insight into the paleo vegetation.

Central and southern Negev speleothems $\delta^{13}\text{C}$ vary between 1.5‰ and -8.4% , which represent general higher values in comparison to the northern Negev and central to northern Israel, where $\delta^{13}\text{C}$ values vary between -9 and -13% . The lower values are interpreted to reflect a dominance of C3 type vegetation and higher values an increase in C4 type vegetation (Vaks et al., 2010, Bar-Matthews et al., 2019). Especially the southern Negev Desert as nearest area with similar environments of the Eastern Desert of Egypt provides an anchor point to interpret our new $\delta^{13}\text{C}$ data pointing to a mixture of C3 and C4.

Following this interpretation, the mean $\delta^{13}\text{C}$ data of MIS 5e points to a higher portion of C3 type vegetation between 127 and 120 ka compared to MIS 5d and 5b, with higher mean $\delta^{13}\text{C}$ values. The archaeobotanical record of the close by Sodmein Cave from layer J, dated to the LIG (Mercier et al., 1999), represents a mixture of C3 and C4 type vegetation with abundant leaf remnants showing the presence of foliages and distinct identification of *Ficus* sp., *Acacia tortilis*, *Clematis* sp., *Balanites* cfr. *Aegyptiaca*, *Paliurus* cfr. *Spina Christi* (Rhamnaceae), *Brassicaceae*, *Gramineae* (Moeyersons et al., 2002). In light of the isotope data, a similar vegetation mixture seems likely for the Saqia Cave, with respective fluctuation in C3/C4 over time. The actual proportions of C3 and C4 type vegetation cannot be quantified, however. The qualitative observation of having the most C3 vegetation during the wet MIS 5e is plausible, but should be verified by more data and approaches to quantify some of the other parameters that potentially affect $\delta^{13}\text{C}$.

The $\delta^{18}\text{O}$ signature from Saqia Cave ($-11,22 \pm 0,29\%$) shows a strong depletion in ^{18}O indicative of a long-distance transport of moisture or at least strong Rayleigh fractionation from the vapour source to the site of precipitation. Similarly, low $\delta^{18}\text{O}$ of $-12,26 \pm 0,18\%$ at Sannur Cave has been interpreted as a “monsoon-signal” in Northeast African precipitation (El-Shenawy et al., 2018). Following this interpretation, the slightly higher values observed at Saqia Cave may be related to the closer proximity to the Red Sea and the possible impact of additional precipitation sources apart from the monsoon. Potential kinetic isotope effects, e.g. due to CO_2 degassing can increase isotopic compositions of speleothems and do not plausibly explain the low $\delta^{18}\text{O}$.

Oxygen signature of southern Negev Desert speleothems (Fig. 3) are in general less depleted in ^{18}O interpreted as higher effect of Eastern Mediterranean moisture, but still with a portion of a tropical, strongly depleted ^{18}O moisture sources (Vaks et al., 2010). There is a clear distinction from the dripstone growth from the central Levant in Soreq Cave (Central Israel), which has a much lighter oxygen isotope in the range of -7 to -3% (Bar-Matthews et al., 2003) and lies within the sphere of influence of the eastern Mediterranean. New data from Soreq Cave reveal a seasonal signal and the influence of a ^{18}O depleted moisture source that increases at certain times of maximum seasonality in precession cycles (Orland et al., 2019). Significant shifts of a varying source of moisture throughout the different sub-stages of MIS 5 are so far not evident for Saqia Cave, as sampling resolution and uncertainties in speleothem growth axes limits a more detailed high-resolution isotope record. However, the possible impact of a varying and divers’ sources of

moisture for the Eastern Desert of Egypt are discussed below after a comparison to a wider spectrum of climate archives in Northeast Africa.

5.2. Northeast Africa in context of human dispersal during MIS 5

In this section, additional non-speleothem based climate proxies for Northeast Africa are considered for the period 60 to 140 ka (Fig. 4), to discuss regional environmental changes and their possible influence for human dispersal throughout Northeast Africa. The few dated speleothem deposits during MIS 6 may be of interest for the discussion of a very early dispersal of *Homo sapiens*, as the oldest fossil of *Homo sapiens* outside of Africa so far is dated to 194-177ka at Misliya Cave in Israel (Hershkovitz et al., 2018). In this context, speleothem growth phases from Saqia Cave at 185.7 ± 4.3 ka and 174.0 ± 4.6 ka, with associated wetter climate in the Eastern Desert of Egypt might suggest ecologically more favorable conditions during a possible early dispersal throughout the SAD. These growth phases are also of interest with regard to postulated wetter climate in the Mediterranean area between 180 and 170 ka and the correlation with the deposition of Sapropel 6 (e.g. Bard et al., 2002). A possibly also older *Homo sapiens* fossil of Apidima Cave in Greece, dated to about 210 ka, is discussed controversially (Harvati et al., 2019). However, most evidence for a dispersal across Northeast Africa exist for MIS 5, for which the majority of speleothem growth phases we have examined provide clear evidences of more humid climate conditions in the Eastern Desert.

African Humid periods during the early late Pleistocene correlate in general with peaks of insolation and an enhanced monsoon activity with a northward shift of the tropical rainfall belt during MIS 5e, 5c and 5a. These large-scale changes at continental scale are also visible in the pronounced growth phases at Saqia Cave, which correlate well with the marine record of Ehrmann et al., (2016), with the African Humid Periods 4 and 3, and with the more general Wet-Dry Index of North-Africa by Grant et al., (2017). In particular, the transition from MIS 5d to 5c and MIS 5b and 5a during the strong increase in insolation show warmer and wetter climate conditions on Northeast Africa. However, the results from Saqia cave reflect speleothem deposits not only during times with a strong increase in insolation, as one of the primary forces for wetter climate in North Africa, but also singular growth phases during times of lower insolation, e.g. the beginning of MIS 5d and the end of MIS 5c. The causes of these phases cannot be fully clarified on the basis of our data, but they may represent a regional peculiarity that can be identified in the future with a better data basis. Here, marine records show only very weak alternations and wetter climate. Both marine records from the Mediterranean Sea and climate models integrate climate fluctuations over larger scales and only partly capture regional characteristics. Hence, the differences observed between our local record and the marine record are most probably related to distinct regional to local terrestrial climate. Understanding local climate fluctuations based on terrestrial archives is essential for understanding the regional environment and the archaeological sites within.

All dated speleothem growth phases of Saqia Cave correlate well with human occupation at Sodmein Cave and certainly it was these more humid climate conditions that made an occupation of the Eastern Desert attractive to humans. The lowermost occupation layer of Sodmein Cave dates between 127.2 ± 3.5 ka to 83.2 ± 2.1 ka (Mercier et al., 1999; Schmidt et al., 2015) and all dates derived from heated flint are within their range of the corresponding speleothem growth phases (Fig. 4 C). In addition, the open-air site Sodmein Playa with stone artefacts of the Early Nubian technology attest LIG occupation (Kindermann et al., 2018).

In the Western Desert of Egypt, there also exists a general agreement with the paleoenvironmental records in context of human occupation during the LIG. Several archaeological sites date back to MIS 5 in context of a wetter climate in the region, e.g. Bir Tarfawi/Bir Sahara (Wendorf et al., 1993; Nicoll, 2018) or Kharga Oasis (Smith et al., 2007). However, the geological context and the landscape patterns in the Western Desert

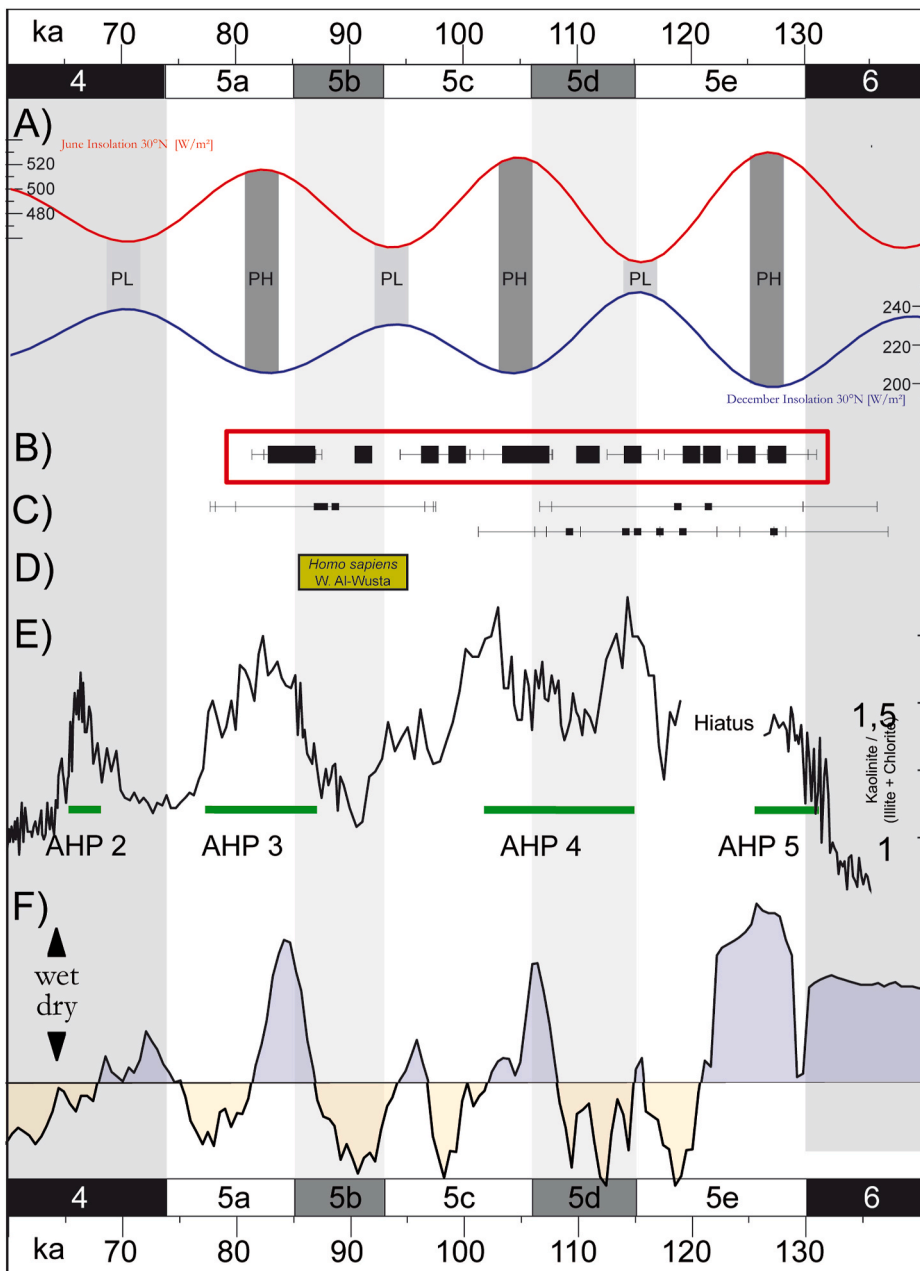


Fig. 4. Selection of palaeoenvironmental records A) Insolation at 25°N (Berger and Loutre, 1991); B) Speleothem growth intervals at Saqia Cave (this study); C) Thermoluminescence dating of heated artefacts from Layer J (MERCIER ET AL., 1999; SCHMIDT ET AL., 2015); D) *Homo sapiens* fossil from Wadi Al Wusta, Saudia Arabia (Groucutt et al., 2018); E) Nile discharge and African Humid Periods 2–5 (Ehrmann et al., 2016); F) Composite wet-dry index for North-African Humid periods (Grant et al., 2017); Marine Isotope stages (MIS) are indicated at the top and bottom according to Railsbeck et al., (2015).

differ fundamentally from the landscape in the Eastern Desert, where large scale palaeohydrological river system did not exist and fluvial-lacustrine environments are almost absent. Most of the archaeological sites in the Western Desert are directly related to large-scale hydrological systems, which could also provide a permanent water sources throughout the year apart from rainfalls. They represent the majority of archives in the Western Desert. Findings of the Nile perch at Bir Tarfawi dating back to the LIG suggest at least a semi-continuous connection of the Nile with the palaeolakes (Van Neer, 1993). For example, Hill and Schild (2017) characterise the deposits at Bir Sahara as wetlands, ponds or small lakes during MIS 5. Several proxies in the oases of Egypt's Western Desert suggest an intermixture of higher rainfalls and rising groundwater tables with activation of spring mounds, where palaeolakes existed at several times during the Late Pleistocene (Blackwell et al., 2017). For the time period of the LIG, direct dated evidences for the activation of the hydrological system exist at Dakhla Oasis (Kleindienst et al., 2008), Kharga Oasis (Smith et al., 2007, Smith et al., 2007; Kleindienst et al., 2008; Blackwell et al., 2017),

and Kurkur Oasis (Crombie et al., 1997). Even though, direct influx of large river systems and surface water discharge is limited, rising groundwater table and outflow is an important water source for the palaeolakes (Kieniewicz and Smith, 2009). Apart from the general geological and hydrological differences between the Western Desert and the Eastern Desert, the different types of topography have a considerable effect on precipitation.

The geographical specifics of the Eastern Desert are enhanced rainfall due to orographic effects of the Red Sea Mountains, the close proximity to the Red Sea, and the overall influence of additional other sources of precipitation apart from the monsoon, which is the superior source of precipitation in the Western Desert. In total, five different precipitation sources could increase annual rainfall during the LIG. The African monsoon during summer months, tropical plums mostly in autumn and winter, the activation of the Red Sea through in spring and autumn, the Mediterranean storm track and cyclones (westerlies) and strong convectional rainfall during winter months (Kutzbach et al., 2014; Skinner and Poulsen, 2015). Hartmann et al., (2020) argue that

the increase in summer precipitation in the northern Red Sea does not only account for the strong fluvial flooding's in the northern Red Sea catchment during MIS 5e, c and a due to strong summer rainfalls, but rather indicate the increased frequency of tropical plums and Red Sea Troughs, as the dominant source of increased precipitation in this region. Waldmann et al. (2010) discusses the possibility for a strong mix up of potential sources in the southern Levant. Here, not only the intensification and southward shift of the Mediterranean westerlies, but also the activation of Red Sea Troughs during shorter wetter periods provide an important moisture source.

Recently, the impact of a strong northward intrusion of the summer monsoon during the LIG (with high seasonal precession) beyond the southern Levant has been suggested for Soreq Cave. Here, the seasonal reconstruction of precipitation sources derived from 18O data from speleothems and concurrent climate modelling point to a tropical moisture source during the summer month during the LIG as an addition to enhanced Mediterranean winter rainfall (Orland et al., 2019). Thus, a northward intrusion of the tropical summer monsoon occurs at a latitude up to 31.7° N, which is also coherent with results from Tzavoa Cave at 31° N and Aslahim Cave at 30° 56' N, where a tropical rainfall component cannot be ruled out during the LIG (Vaks et al. 2006, 2017).

The in-depth comparison of different climate models of the LIG for the Arabian Peninsula and Northeast Africa presented by Jennings et al. (2015) reach similar conclusions, that during distinct phases of the LIG, e.g. at 125 ka, the tropical summer monsoon reached maximal far north up to 34° N (COSMOS and CCSM3), 29° N (KCM), 28° N (NorESM) or up to a minimum extension up to 23° N (HadCM3). Hereby, the comparison with paleoclimate records point to evidences, that the more humid models, respectively the more northern position of the tropical monsoon, give most realistic scenarios (Jennings et al., 2015). With regard to all these evidences from various kind of archives and climate modelling, the very depleted $\delta^{18}\text{O}$ values from Saqia Cave confirms the main influence of a tropical moisture source. This interpretation and mechanism of depleted $\delta^{18}\text{O}$ values as indicator for a long distance transport of a tropical moisture source in Northeast Africa during the LIG is also in line with the ECHAM4 general circulation model (Herold and Lohmann, 2009). Hence, Saqia Cave reveals additional proofs for a northward intrusion of the tropical monsoon during phases of the LIG to a northern latitude of at least 26° N.

In particular, the in-phase intensification of the northward shift of the summer monsoon with the congruent southward shift of the winter Mediterranean rainfall zone during phases of large Precession High's led to the overlap of these precipitation regimes with periodically interaction between 30° N and 25° N in northeastern Africa (Kindermann et al., 2006; Kutzbach et al., 2014). Saqia Cave, located at 26° N at this transition and overlap zone, shows speleothem growth over all LIG phases of enhanced precession high. Thus, contribution from winter rainfall Mediterranean storm tracks as well as summer rainfall from the monsoon regime is likely.

The additional influence of Red Sea Troughs is spatially limited to the mountainous areas east of the Nile Valley as the mostly flat region west of the Nile Valley do not force topographically induced rainfall. Thus, a considerable west to east precipitation gradient exists in Egypt, with possible wetter climate conditions in the eastern part and adjacent regions of the Red Sea (Saqia Cave only 25 km direct distance to the Red Sea) in contrast to the western regions (e.g. Bir Tarfawi around 700 km distance to the Red Sea). This hypothesis should be strengthened during future work and testifies to the fact that more archives are needed for an in-depth comparison of precipitation variability at regional scale. However, this also means that difficult and complex archives must be used, such as our example. Otherwise, for the time slice of interest and for such a hyper arid region, there are hardly any straightforward interpretable terrestrial archives.

The close distance of the Eastern Desert to the proposed palaeohydrological corridor for hominin dispersal ("Tabuk corridor") in Northeast Arabia (Breeze et al., 2016) is relevant to compare the

situation with focus on the eastern part of Egypt as a possible important corridor. The so far only Pleistocene *Homo sapiens* fossil found on the Arabian Peninsula at Wadi Al Wusta dates back to around 95–86 ka (Groucutt et al., 2018). The site is located on a similar latitude as Saqia Cave (Wadi Al Wusta 27° 25' N, Saqia Cave 26° 19' N) and wetter climate conditions are also proposed for the time of the human occurrence, which are documented through the peak of insolation at around 84 ka (Groucutt et al., 2018). Altogether, this highlights that the adjacent regions of the Red Sea, on both sides in Northeast Africa and on the Arabian Peninsula, narrows down a more specific region of interest at the natural topographic bottleneck for the dispersal of *Homo sapiens* during the LIG.

6. Conclusion

Given the complexity of possible synoptic atmospheric interactions during the LIG and multiple explanations for an increase in precipitation in Northeast Africa, it is evident that the actual climatological and environmental setting is regionally highly diverse. Therefore, it is very important to discuss not only palaeoenvironments in Northeast Africa at large scales, but also the various regional environments and the influence on possible human mobility. The new speleothem record of Saqia Cave enlarges the available climate records in this region and allows a spatially more diverse consideration of environmental changes. The integration of Saqia Cave, located in the most central part of the nowadays arid barrier between the tropical and temperate climate system, represents the dominant tropical moisture source, reflected in the $\delta^{18}\text{O}$ values, but also confirms the strong interaction of the tropical and temperate climate system during the LIG. It indicates that the wetter climate of the Eastern Desert of Egypt during MIS 5 is not only caused by a strong northward shift of the African monsoon during peaks of insolation during MIS 5e, c and a, but also during the intermediate phases of less insolation. The relative close location to the Red Sea, the possible influence of tropical plumes and the southward shift of the Mediterranean rainfall zone apart from the strong influence of the African and Indian monsoon can explain wetter climate conditions in the region before and after a strong increase and peak of insolation during the LIG. The identification of a diverse regional precipitation pattern in this part of Northeast Africa gives new impetus to the discussion of the relevance of favorable environmental regions to human dispersal. The results suggest that the Eastern Desert of Egypt could have served as a possible humid corridor during the LIG. These favorable climate conditions provided an essential basis for the recurrent human occupation during the Late Pleistocene in the Sodmein region. Although our speleothem site faces several challenges as discussed, it provides a new record to identify phases of past local to regional enhanced precipitation in the past.

The general existing of speleothem growth phases throughout all sub-stages of MIS 5 demonstrates the high potential of further sampling at Saqia Cave for better chronology and in-depth information on precipitation sources using the $\delta^{18}\text{O}$ signature, the $\delta^{13}\text{C}$ -deduced variation in the portion of C3 and C4 type vegetation, but also additional paleoenvironmental information based on fluid inclusion or more geochemical proxies. Given the so far very rare presence of speleothem deposits in Egypt covering the LIG, the new terrestrial archive from Saqia Cave, in particular with its close spatial context to Sodmein Cave, is an extraordinary source of information to study human-environment interaction and thus also for the dispersal of *Homo sapiens* OoA.

Author contribution

Conceptualization: FH, KK, OB; Fieldwork: FH, RE, AA, KK, OB; Laboratory and data analysis: FH, RE, ASR, DH, NF; Funding acquisition: KK, OB. Writing initial draft: FH with contributions from all authors. All authors have reviewed and edited the final manuscript.

Data availability

The authors confirm that the data supporting the findings of this study are available within the article and its supplementary materials.

Declaration of competing interest

The authors declare that they have no known competing financial interests or personal relationships that could have appeared to influence the work reported in this paper.

Acknowledgments

This study is part of the Collaborative Research Centre 806 “Our Way to Europe”, subproject A1 “Out of Africa – Late Pleistocene Rock Shelter Stratigraphies and Palaeoenvironments in Northeast Africa”, (funded grant number 57444011 – SFB 806) by the Deutsche Forschungsgemeinschaft (DFG). We thank the Egyptian Mineral and Resources Authority (EMRA) for providing help during fieldwork and exporting the samples. We thank the student assistants at IUP for chemical preparation of Th/U samples and Augusto Mangini for his initial cooperation with IUP. Christina Montana Puscas helped us with previous isotope measurements. Finally, we would like to thank Mathias Ritter, who discovered the flowstone during a geoarchaeological survey. The comments and suggestions for improvement made by two reviewers are thanked, as is the work of the editors.

Appendix A. Supplementary data

Supplementary data to this article can be found online at <https://doi.org/10.1016/j.quaint.2021.05.006>.

References

- Bajo, P., Borsato, A., Drysdale, R., Hua, Q., Frisia, S., Zanchetta, G., Hellstrom, J., Woodhead, J., 2017. Stalagmite carbon isotopes and dead carbon proportion (DCP) in a near-closed-system situation: an interplay between sulphuric and carbonic acid dissolution. *Geochim. Cosmochim. Acta* 210, 208–227. <https://doi.org/10.1016/j.gca.2017.04.038>.
- Bard, E., Delaygue, G., Rostek, F., Antonioli, F., Silenzi, S., Schrag, D.P., 2002. Hydrological conditions over the western Mediterranean basin during the deposition of the cold Sapropel 6 (ca. 175 kyr BP). *Earth Planet. Sci. Lett.* 202, 481–494. [https://doi.org/10.1016/S0012-821X\(02\)00788-4](https://doi.org/10.1016/S0012-821X(02)00788-4).
- Braun, K., Nehme, C., Pickering, R., Rogerson, M., Scroxton, N., Harrison, S.P., Comas-Bru, L., 2019. A window into africa's past hydroclimates: the SISAL_v1 database contribution. *Quaternary* 2 (1). <https://doi.org/10.3390/quat2010004>.
- Bar-Matthews, M., Ayalon, A., Gilmour, M., Matthews, A., Hawkesworth, C.J., 2003. Sealand oxygen isotopic relationships from planktonic foraminifera and speleothems in the Eastern Mediterranean region and their implication for paleorainfall during Interglacial intervals. *Geochim. Cosmochim. Acta* 67, 3181–3199. [https://doi.org/10.1016/S0016-7037\(02\)01031-1](https://doi.org/10.1016/S0016-7037(02)01031-1).
- Bar-Matthews, M., Keinan, J., Ayalon, A., 2019. Hydro-climate research of the late quaternary of the Eastern Mediterranean-Levant region based on speleothems research – a review. *Quat. Sci. Rev.* 221 <https://doi.org/10.1016/j.quascirev.2019.105872>.
- Blackwell, B.A.B., Skinner, A.R., Smith, J.R., Hill, C.L., Churcher, C.S., Kieniewicz, J.M., Adelsberger, K.A., Blickstein, J.I.B., Florentin, J.A., Deely, A.E., Spillar, K.V., 2017. ESR analyses for herbivore teeth and molluscs from Kharga, dakhleh, and Bir Tarfawi oases: constraining water availability and hominin paleolithic activity in the Western Desert, Egypt. *J. Afr. Earth Sci.* 136, 216–238. <https://doi.org/10.1016/j.jafrearsci.2017.07.007>.
- Breeze, P., Groucutt, H.S., Drake, N.A., White, T.S., Jennings, R.P., Petraglia, M.D., 2016. Palaeohydrological corridors for hominin dispersals in the Middle East ~250–70,000 years ago. *Quat. Sci. Rev.* 144, 155–185. <https://doi.org/10.1016/j.quascirev.2016.05.012>.
- Brook, G., Embabi, N.S., Ashour, M., Edwards, R., Cheng, H., Cowart, J., Dabous, A., 2002. Djara cave in the Western Desert of Egypt. Morphology and evidence of quaternary climatic change. *Cave Karst Sci.* 29 (2), 57–66.
- Burns, S.J., Matter, A., Frank, N., Mangini, A., 1998. Speleothem-based paleoclimate record from northern Oman. *Geology* 26 (6), 499–502.
- Burns, S.J., Fleitmann, D., Matter, A., Neff, U., Mangini, A., 2011. Speleothem evidence from Oman for continental pluvial events during interglacial periods. *Geology* 29 (7), 623–626.
- Burstyn, Y., Martrat, B., Lopez, J.E., Iriarte, E., Jacobson, M.J., Lone, M.A., Deininger, M., 2019. Speleothems from the Middle East: an example of water limited environments in the SISAL database. *Quaternary* 2 (16). <https://doi.org/10.3390/quat2020016>.
- Cheng, H., Edwards, R.L., Hoff, J., Gallup, C.D., Richards, D.A., Asmer-om, Y., 2000. The half-lives of uranium-234 and thorium-230. *Chem. Geol.* 169, 17–33.
- Conoco, 1987. Geological Maps of Egypt. 1:500,000. Conoco Coral and the Egyptian General Petroleum Corporation, Cairo.
- Crombie, M.K., Arvidson, R.E., Sturchio, N.C., El Alfy, Z., Abu Zeid, K., 1997. Age and isotopic constraints on Pleistocene pluvial episodes in the Western Desert, Egypt. *Paleogeography, Paleoclimatology, Paleoecology* 130, 337–355. [https://doi.org/10.1016/S0031-0182\(96\)00134-4](https://doi.org/10.1016/S0031-0182(96)00134-4).
- Dabous, A., Osmond, J., 2000. U/Th isotopic study of speleothems from the wadi Sannur cavern, Eastern Desert of Egypt. *Carbonates Evaporites* 15 (1), 1–6.
- Douville, E., Salle, E., Frank, N., Eisele, M., Pons-Branchu, E., Ayrault, S., 2010. Rapid and accurate U-Th dating of ancient carbonates using inductively coupled plasma-quadrupole mass spectrometry. *Chem. Geol.* 272, 1–11. <https://doi.org/10.1016/j.chemgeo.2010.01.007>.
- Ehrmann, W., Schmiedl, G., Seidel, M., Krüger, S., Schulz, H., 2016. A distal 140 kyr sediment record of Nile discharge and East African monsoon variability. *Clim. Past* 12, 713–727. <https://doi.org/10.5194/cp-12-713-2016>.
- El-Asrag, A.M., 2005. Effect of Synoptic and Climatic Situations on Fractionation of Stable Isotopes in Rainwater over Egypt and East Mediterranean (IAEA-TECDOC-1453). International Atomic Energy Agency (IAEA).
- El-Shenawy, M., Kim, S.-T., Schwarcz, H., Asmerom, Y., Polyak, V., 2018. Speleothem evidence for the greening of the Sahara and its implications for the early human dispersal out of sub-Saharan Africa. *Quat. Sci. Rev.* 188, 67–76.
- Fleitmann, D., Burns, S.J., Neff, U., Mangini, A., Matter, A., 2003. Changing moisture sources over the last 330,000 years in the Northern Oman from fluid-inclusion evidence in speleothems. *Quat. Res.* 60, 223–232.
- Fleitmann, D., Burns, S.J., Pekala, M., Mangini, A., Al-Subbary, A., Al-Aowah, M., Kramers, J., Matter, A., 2011. Holocene and Pleistocene pluvial periods in Yemen, southern Arabia. *Quat. Sci. Rev.* 30, 783–787.
- Ford, D., Williams, P., 2007. *Karst Hydrogeology and Geomorphology*. John Wiley & Sons, West Sussex, p. 562.
- Frank, N., Braun, M., Hambach, U., Mangini, A., Wagner, G., 2000. Warm-period growth of travertine during the last interglaciation in southern Germany. *Quat. Res.* 54, 38–48.
- Grant, K.M., Rohling, E.J., Bar-Matthews, M., Ayalon, A., Medina-Elizalde, M., Bronk-Ramsey, C., Satow, C., Roberts, A.P., 2012. Rapid coupling between ice column and polar temperature over the past 150,000 years. *Nature* 491, 744–747. <https://doi.org/10.1038/nature11593>.
- Grant, K.M., Rohling, E.J., Westerhold, T., Zabel, M., Heslop, D., Konijnendijk, T., Lourens, L., 2017. A 3 million year index for North African humidity/aridity and the implication of potential pan-African humid periods. *Quat. Sci. Rev.* 171, 100–118. <https://doi.org/10.1016/j.quascirev.2017.07.005>.
- Groucutt, H.S., Grün, R., Zalmout, I.A.S., Drake, N.A., Armitage, S.J., Candy, I., Clark-Wilson, R., Louys, J., Breeze, P.S., Duval, M., Buck, L.T., Kivell, L.L., Pomeroy, E., Stephens, N.B., Stock, J.T., Stewart, M., Price, G.J., Kinsley, L., Tong, W.W., Alsharakh, A., Al-Omari, A., Zahir, M., Memesh, A.M., Abdolshakoor, A.J., Al-Masari, A.M., Bahameem, A.A., Al Murayy, K.M.S., Zahrani, B., Scerri, E.L.M., Petraglia, M.D., 2018. *Homo sapiens* in Arabia by 85,000 years ago. *Nature Ecology & Evolution*. <https://doi.org/10.1038/s41559-018-0518-2>.
- Hartmann, A., Torfstein, A., Almogi-Labin, A., 2020. Climate Swings in the northern Red Sea over the last 150,000 years from eNd and Mg/Ca of marine sediments. *Quat. Sci. Rev.* 231 <https://doi.org/10.1016/j.quascirev.2020.106205>.
- Harvati, K., Röding, C., Bosman, A.M., Karakostas, F.A., Grün, R., Stringer, C., karkanis, P., Thompson, N.C., Koutoulidis, V., Moulououlos, L.A., Gorgoulis, V.G., Kouloukoussa, M., 2019. Apidima Cave fossils provide earliest evidence of *Homo sapiens* in Eurasia. *Nature* 571, 500–504. <https://doi.org/10.1038/s41586-019-1376-z>.
- Herold, M., Lohmann, G., 2009. Eemian tropical and subtropical African moisture transport: an isotope modelling study. *Clim. Dynam.* 33, 1075–1088. <https://doi.org/10.1007/s00382-008-0515-2>.
- Hershkovitz, I., Weber, G.W., Quam, R., Duval, M., Grün, R., Kinsley, L., Ayalon, A., Bar-Matthews, M., Valladas, H., Mercier, N., Arsuaga, J.L., Martinon-Torres, de Castro, J. M., Fornai, C., Maartin-Frances, L., Sarig, R., May, H., Krenn, V.A., Slon, V., Rodriguez, L., Garcia, R., Lorenzo, C., Carretero, J.M., Frumkin, A., Shahack-Gross, R., Bar-Yosef Mayer, D.E., Cui, Y., Whu, X., Peled, N., Groman-Yaroslavski, I., Weissbrod, L., Yeshrum, R., Tsatskin, A., Zaidner, Y., Weinstein-Evron, M., 2018. The earliest modern humans outside Africa. *Science* 359, 456–459. <https://doi.org/10.1126/science.aap8369>.
- Hill, C., Schild, R., 2017. Paleohydrology and paleoenvironments at Bir Sahara. Pleistocene lithostratigraphy and sedimentology in the southern Egyptian Sahara. *J. Afr. Earth Sci.* 136, 201–2015. <https://doi.org/10.1016/j.jafrearsci.2017.02.031>.
- Jennings, R.P., Singarayer, J., Stone, E.J., Krebs-Kanzow, U., Khon, V., Nisanoglu, K.H., Pfeiffer, M., Zhang, X., Parker, A., Parton, A., Groucutt, H.S., White, T.S., Drake, N. A., Petraglia, M.D., 2015. The greening of Arabia: multiple opportunities for human occupation of the Arabian Peninsula during the Late Pleistocene inferred from an ensemble of climate simulations. *Quat. Int.* 382, 181–199.
- Khalil, S.M., McClay, K.R., 2002. Extensional fault-related folding, northwestern Red Sea, Egypt. *J. Struct. Geol.* 24, 743–762.
- Kieniewicz, J.M., Smith, J.R., 2009. Paleoenvironmental reconstruction and water balance of a mid-Pleistocene pluvial lake, Dakhleh Oasis, Egypt. *GSA Bulletin* 121 (7/8), 1154–1171. <https://doi.org/10.1130/B26301.1>.
- Kindermann, K., Bubenzer, O., Nussbaum, S., Riemer, H., Darius, F., Pöllath, N., Smettan, U., 2006. Palaeoenvironment and Holocene land use of Djara, Western Desert of Egypt. *Quat. Sci. Rev.* 25 (13–14), 1619–1637. <https://doi.org/10.1016/j.quascirev.2005.12.005>.

- Kindermann, K., Van Peer, P., Henselowsky, F., 2018. At the lakeshore – an Early Nubian Complex site linked with lacustrine sediments (Eastern Desert, Egypt). *Quat. Int.* 485, 131–139. <https://doi.org/10.1016/j.quaint.2017.11.006>.
- Kleindienst, M.R., Schwarcz, H.P., Nicoll, K.A., Churcher, C.S., Frizano, J., Giegengack, R., Wisemann, M.F., 2008. Water in the Desert: first report on uranium-series dating of caton-Thompson's sequence at refug pass, Kharga Oasis. In: Wisemann, M.F. (Ed.), *The Oasis Papers 2. Proceedings of the Second International Conference of the Dakhleh Oasis Project*. Oxbow Books, Oxford, pp. 25–54.
- Kutzbach, J.E., Chen, G., Cheng, H., Edwards, R.L., Liu, Z., 2014. Potential role of winter rainfall explaining increased moisture in the Mediterranean and Middle East during periods of maximum orbitally-forced insolation seasonality. *Clim. Dynam.* 42, 1079–1095. <https://doi.org/10.1007/s00382-013-1692-1>.
- Ludwig, K.R., Titterton, D.M., 1994. Calculation of $^{230}\text{Th}/\text{U}$ isochrons, ages, and errors. *Geochem. Cosmochim. Acta* 58 (22), 5031–5042.
- Meier-Augenstein, W., Schimmelmann, A., 2019. A guide for proper utilisation of stable isotope reference materials. *Isot. Environ. Health Stud.* 55 (2), 113–128. <https://doi.org/10.1080/10256016.2018.1538137>.
- Mercier, N., Valladas, H., Froget, L., Joron, J.-L., Vermeersch, P.-M., Van Peer, P., Moeyersons, J., 1999. Thermoluminescence dating of a middle palaeolithic occupation at Sodmein cave, Red Sea Mountains (Egypt). *J. Archaeol. Sci.* 26, 1339–1345.
- Moeyersons, J., Vermeersch, P.M., Van Peer, P., 2002. Dry cave deposits and their palaeoenvironmental significance during the last 115 ka, Sodmein Cave, Red Sea Mountains, Egypt. *Quat. Sci. Rev.* 21, 837–851.
- Nicoll, K., 2018. A revised chronology for Pleistocene paleolakes and middle stone age – middle paleolithic cultural activity at Bir Tarfawi – Bir Sahara in the Egyptian Sahara. *Quat. Int.* 463, 18–28. <https://doi.org/10.1016/j.quaint.2016.08.037>.
- Orland, I.J., He, F., Bar-Matthews, M., Chen, G., Ayalon, A., Kutzbach, J.E., 2019. Resolving seasonal rainfall changes in the Middle East during the last interglacial period. *Proc. Natl. Acad. Sci. Unit. States Am.* <https://doi.org/10.1073/pnas.1903139116>.
- Railsback, L.B., Gibbard, P.L., Head, M.J., Voarintsoa, N., Toucanne, S., 2015. An optimized scheme of lettered marine isotope substages for the last 1.0 million years. *Quat. Sci. Rev.* 111, 94–106. <https://doi.org/10.1016/j.quascirev.2015.01.012>.
- Rohling, E.J., Marino, G., Grant, K.M., 2015. Mediterranean climate and oceanography, and the periodic development of anoxic events (sapropels). *Earth Sci. Rev.* 143, 62–97.
- Sawires, R., Pelaez, J.A., Ibrahim, H.A., Fat-Helbary, R.E., Henaes, J., Hamdache, M., 2016. Delineation and characterization of a new seismic source model for seismic hazard studies in Egypt. *Nat. Hazards* 80, 1823–1864. <https://doi.org/10.1007/s11069-015-2034-x>.
- Schmidt, C., Kindermann, K., van Peer, P., Bubenzer, O., 2015. Multi-emission luminescence dating of heated chert from the middle stone age sequence at Sodmein cave (Red Sea Mountains, Egypt). *J. Archaeol. Sci.* 63, 94–103.
- Skinner, C.B., Poulsen, C.J., 2015. The role of fall season tropical plumes in enhancing Saharan rainfall during the African Humid Period. *Geophys. Res. Lett.* 43 (1), 349–358. <https://doi.org/10.1002/2015GL066318>.
- Smith, J.R., Hawkins, A.L., Asmerom, Y., Polyak, V., Giegengack, R., 2007. New age constraints on the middle stone age occupations of Kharga Oasis, Western Desert, Egypt. *J. Hum. Evol.* 52, 690–701.
- Van Neer, W., 1993. Fish remains from the last interglacial at Bir Tarfawi (eastern Sahara, Egypt). In: Wendorf, F., Schild, R., Close, A.E. (Eds.), *Egypt during the Last Interglacial*. Plenum Press, New York, pp. 144–154.
- Vaks, A., Bar-Matthews, M., Ayalon, A., Matthews, A., Frumkin, A., Dayan, U., Halicz, L., Almogi-Labin, A., Schilman, B., 2006. Paleoclimate and location of the border between the Mediterranean climate region and the Sahara-Arabian Desert as revealed by speleothems from the northern Negev Desert, Israel. *Earth Planet Sci. Lett.* 249, 384–399. <https://doi.org/10.1016/j.epsl.2006.07.009>.
- Vaks, A., Bar-Matthews, M., Ayalon, A., Matthews, A., Frumkin, A., 2007. Desert speleothem reveal climatic window for African exodus of early modern humans. *Geology* 35 (9), 831–834.
- Vaks, A., Bar-Matthews, M., Matthews, A., Ayalon, A., Frumkin, A., 2010. Middle-late quaternary paleoclimate of northern margins of the Sahara-Arabian Desert-reconstruction from speleothems of Negev Desert, Israel. *Quat. Sci. Rev.* 29, 2647–2662.
- Vaks, A., Bar-Matthews, M., Ayalon, A., Matthews, A., Frumkin, A., 2017. Pliocene-pleistocene paleoclimate reconstruction from ashalim cave speleothems, Negev Desert, Israel. In: Arise, M., Gabrovsek, F., Kaufmann, G., Ravbar, N. (Eds.), *Advances in Karst Research: Theory, Fieldwork and Applications*. Geological Society, London, Special Publications, p. 466. <https://doi.org/10.1144/SP466.10>.
- Wefing, A.M., Arps, J., Blaser, P., Wienberg, C., Hebbeln, D., Frank, N., 2017. High precision U-series dating of scleractinian cold-water corals using an automated chromatographic U and Th extraction. *Chem. Geol.* 475, 140–148. <https://doi.org/10.1016/j.chemgeo.2017.10.036>.
- Wendorf, F., Schild, R.S., Close, A.E., 1993. *Egypt during the Last Interglacial. The Middle Paleolithic of Bir Tarfawi and Bir Sahara East*. Plenum Press, New York.
- Yousif, M., Sracek, O., 2016. Integration of geological investigations with multi-GIS data layers for water resources assessment in arid regions: El Ambagi Basin, Eastern Desert, Egypt. *Environ Earth Science* 75, 684. <https://doi.org/10.1007/s12665-016-5456-1>.
- Yousif, M., Henselowsky, F., Bubenzer, O., 2018. Palaeohydrology and its impact on groundwater in arid environments: Gebel Duwi and its vicinities, Eastern Desert, Egypt. *Catena* 171, 29–42. <https://doi.org/10.1016/j.catena.2018.06.028>.